

## Special Article

# Artifacts Associated with MR Neuroangiography

Jay Tsuruda,<sup>1,3</sup> David Saloner,<sup>2</sup> and David Norman<sup>1</sup>

Neurovascular MR angiography (MRA) is rapidly gaining greater clinical acceptance. To provide functional information, novel techniques of acquisition, information processing, and display are used, generating a new set of artifacts. The purpose of this paper is to outline the causes, provide examples, and note clinical problems associated with MRA artifacts by grouping them into six common types: 1) poor visualization of small vessels, 2) overestimation of stenosis, 3) view-to-view variations, 4) false positives, 5) false negatives, and 6) vessel overlap. This in turn will lead to four generalized solutions: 1) optimize acquisition parameters, 2) edit volume boundaries before performing maximum intensity projection reconstructions, 3) refer to the individual source images, and 4) use alternative image processing. By organizing and simplifying both clinical problems and solutions into major categories, a greater understanding of the current clinical indications and the overall goals of MRA can be achieved.

**Index terms:** Magnetic resonance, artifacts; Magnetic resonance angiography (MRA)

AJNR 13:1411–1422, Sep/Oct 1992

Depiction of vascular anatomy by magnetic resonance (MR) imaging has shown rapid advances over the past few years because of the introduction of flow sensitive sequences, which are available on most commercial MR scanners. These sequences are usually derived from either two- or three-dimensional Fourier transformation (2DFT or 3DFT) thin-section gradient recalled echo (GRE) data sets (1–4). These sequences generate signal from moving protons with relative suppression of stationary tissue. The resulting image(s) can be viewed as individual thin sections or reprojected in the form of MR flow maps or MR angiograms (MRA).

MRA of the neck and brain can render excellent depiction of vascular anatomy (5, 6). Preliminary reports have shown promising results in the non-

invasive detection of carotid bifurcation stenosis (7–10), intracranial aneurysms (11, 12), dural sinus occlusion (13), and arteriovenous malformations (14). Despite the initial success of this technique and its impending widespread routine clinical application, little has been said of the potential artifacts and pitfalls of this new technique (15, 16). Some of these problems can be attributed to the fact that MRA actually represents a physiologic map of flow from which anatomic information can be inferred. Accurate representation of this flow information may be less than optimal due to 1) limitations inherent to the MRA acquisition or 2) reconstruction artifacts due to the use of the maximum intensity projection (MIP) algorithm.

To understand the genesis of MRA artifacts, a brief review of the basics of image contrast, image reconstruction, and signal loss with MRA is required. Most of the schemes to produce flow-sensitive MR images are based either on differences in longitudinal magnetization (inflow or time-of-flight) (1, 4, 17–19) or transverse magnetization (phase shift or velocity dephasing/rephasing) (2, 20, 21). The sequences that are commercially available include 2DFT and 3DFT time-of-flight (TOF) and 2DFT and 3DFT phase-contrast (PC) GRE acquisitions. In all of these schemes, the goal is to maximally suppress the intensity of background stationary spins without

---

Received August 8, 1991; accepted and revision requested November 20; revision received on December 18.

Paper presented at the 1990 Annual Meeting of the Western Neuro-radiologic Society, Santa Fe, NM.

<sup>1</sup> Department of Radiology, Diagnostic and Interventional Neuroradiology Section, University of California, San Francisco.

<sup>2</sup> Department of Radiology, Veterans Administration Hospital San Francisco and University of California, San Francisco.

<sup>3</sup> Address reprint requests to Jay Tsuruda, MD, Department of Radiology, SB-05, University of Washington Medical Center, Seattle, WA 98195.

AJNR 13:1411–1422, Sep/Oct 1992 0195-6108/92/1305-1411

© American Society of Neuroradiology



significantly affecting the relatively high signal intensity of flowing blood. The information from a flow-sensitive sequence can be displayed as individual reconstructed 2DFT sections or 3DFT partitions. These sections or partitions have also been called "source" images, since they represent the data that has not been manipulated by image-processing algorithms as discussed below.

To approximate a catheter angiogram-like projection image, all or portions of the individual source images can be projected onto a two-dimensional planar view in any preselected viewing angle. Not only do these projections resemble a conventional angiogram, they also facilitate visualization of tortuous vessels that may be difficult to trace on the individual source images.

Currently, the most commonly commercially used projection algorithm is based on the MIP using a ray-tracing technique (22, 23). The advantages of this technique include: adequate background suppression in most instances and ease of implementation and speed of application, since it is a relatively simple algorithm without extensive requirements of computer memory or processing power.

In practice, a collapsed view and reprojected views are routinely generated from source images (Fig. 1, image 1). The "collapsed" view is obtained by setting the ray-tracing direction perpendicular to all the source images. For example, if multiple axial projections are obtained through the circle of Willis, an image simulating a catheter angiogram submental-vertex projection is generated. A similar projection of the carotid and vertebral arteries can be obtained from axial neck MRA images (Fig. 1, image 2). The "reprojected" views are obtained by setting the ray-tracing direction parallel to the plane of the source images. For example, from the original axial data set of the neck, one can obtain a lateral reprojection (Fig. 1, image 3). Simply rotating the direction of the ray will yield additional oblique and anterior-posterior reprojections. By obtaining multiple reprojected images, a cinegraphic display demonstrating a region of interest rotating in space can be viewed on the display station monitor. This rotational display may assist in understanding complex three-dimensional vascular anatomy or regions of vessel irregularity such as ulceration.

The two major mechanisms of signal loss are slow flow and disturbed flow (spin dephasing) (24, 25). Since the source of signal contrast is the movement of flowing blood, with diminishing flow rates blood will more closely approximate the

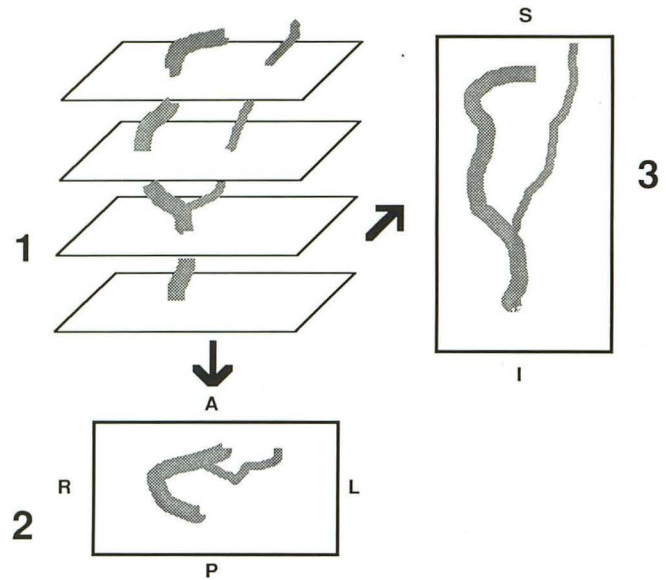


Fig. 1. Methods of MRA image display. In this diagram, a simplified MRA through the carotid artery was obtained using four axial gradient recalled images. This information can be displayed as three basic types of images: 1) source, 2) collapsed, and 3) reprojection. The source images are the individual sections obtained from the original acquisition. The collapsed image is obtained by performing a maximum intensity projection (MIP) perpendicular to the source images, as indicated by the arrow. In this example, since the source images were oriented in the axial plane, the collapsed view is equivalent to a submental-vertex projection. The reprojection is obtained by performing the MIP parallel to the source image. In this example, a lateral view is shown.

appearance of stationary tissue. The term "saturation effect" has been used to describe this phenomenon with TOF MRA (26).

Signal loss in disturbed flow states occurs because MRA methods are devised to generate high signal strength for voxels containing protons that have moved with constant velocity in the interval between radiofrequency (RF) excitation and signal acquisition (17). In certain normal and pathologic vascular conditions however, flow patterns are generated in which the blood no longer exhibits linear streamlines. The most common example is at regions immediately distal to stenosis where a high velocity flow jet enters a region of poststenotic dilatation. Even in normal vessels, flow separation, including recirculating flow, may occur. This phenomenon often occurs at vessel bifurcations such as the common carotid artery, the terminal segment of the internal carotid artery, and basilar tip, as well as in vessels with a normally tortuous course such as the carotid siphon (27, 28). In both instances, protons have undergone accelerative and higher order motion. When evaluated by MRA, there is incorrect en-



coding of the magnetization strength and/or incoherent phase shifting within the imaging voxel at the site of disturbed flow resulting in signal dropout. Stenosis, therefore, is typically overestimated, the signal intensity in the carotid artery is uneven, and the diameter of the vascular lumen is underestimated.

High signal in MRA images derives from blood flowing into the region of interest, independent of the direction of flow. Lack of discrimination between arteries and veins results in a complex image that is difficult to interpret. A variety of solutions are employed depending on whether TOF or PC techniques are used. For example, the use of superiorly positioned RF saturation bands will reduce signal in the jugular vein when performing TOF MRA of the neck (29). PC MRA data can be reconstructed such that the direction of flow can be determined, thus providing a physiologic basis for distinguishing between vessels. In addition, image-processing techniques that allow selective editing of the sample volume before reconstruction as well as rotational display can be employed to sort out complex anatomy.

Despite attempts by the manufacturer to address some of the potential causes of artifacts by optimizing acquisition software, correcting eddy currents, improving RF coil design, and developing user friendly displays, artifacts will invariably occur. Several different approaches can be taken to classify these potential artifacts and limitations. The first is to list the numerous causes of image degradation as outlined in Table 1. This list consists of two major categories: 1) subject variability

TABLE 1: Causes of MRA artifacts

I. Subject variability
Normal and abnormal blood flow
Slow flow or secondary recirculation
Higher order motion (nonlinear flow, turbulence, accelerated flow, nonconstant flow, etc)
Streamline flow
Motion (vessel wall or patient)
Local field inhomogeneities
Soft-tissue (background) variability
II. Data acquisition, image processing and display
Acquisition parameters
TR, TE, flip angle, velocity encoding, and compensation
Voxel resolution
Vessel overlap
Misregistration
Partial voluming
Truncation errors
Fourier versus partial Fourier reconstruction
Maximum intensity projection algorithm

and 2) data acquisition, processing, and display. A detailed description on how each of these points may have an impact on the MRA can then be pursued. From a practical standpoint, the various causes for image degradation will not occur in isolation. An alternative approach is to categorize the cumulative effect of artifacts as clinical problems that may lead to misinterpretation. We will take the later approach and illustrate common examples of each of the major clinical problems as well as describe individual sources that can be adopted on a routine basis.

### Artifact Examples

For simplification, there are six specific clinical problems that can be commonly generated on clinical MRA studies\*: 1) poor visualization of small vessels, 2) overestimation of stenosis, 3) view-to-view variations, 4) false positives, 5) false negatives, and 6) vessel overlap. In the following section, selected clinical cases are shown to illustrate each of these types.

#### *Poor Visualization of Small Vessels*

As noted in the introduction, viewing the MIP collapsed and reprojected views have certain advantages. Unfortunately, vascular anatomy can be systematically distorted. The reason is simple: whenever the MIP algorithm is performed to produce either a collapsed or reprojected view, unusual contrast behavior can be present. The exact mechanism has been described in detail (15, 30). Briefly, the successful implementation of the MIP algorithm can be depicted as a statistical function. For the MIP to have a high probability of success, the intensity of the vessel should be on the average at least 2 standard deviations above background intensity. Remember, the ray-tracing technique is designed to depict only the maximum intensity encountered as the ray passes through the imaging volume. It is to be hoped that the highest intensity voxel represents flowing blood.

There will be a greater statistical chance of failure using this algorithm in adequately depicting a vessel when several conditions are present.

\* All patient studies were performed on 1.5-T units (Magnetom, Siemens AG, Erlangen, Germany; Signa, General Electric Medical Systems, Milwaukee, WI). Standard production coils were used for both cranial and neck MRA. TOF and PC MRA were performed using techniques that have been previously described (2, 4, 5, 8, 11, 12, 13, 21).



First, if the signal intensity of the vessel decreases due to partial voluming, reduced vessel velocity or saturation effects, the MIP will underestimate its size. This problem can be commonly seen in depicting small vessels in a collapsed view of the circle of Willis (Fig. 2). In some cases, the vessel may actually disappear.

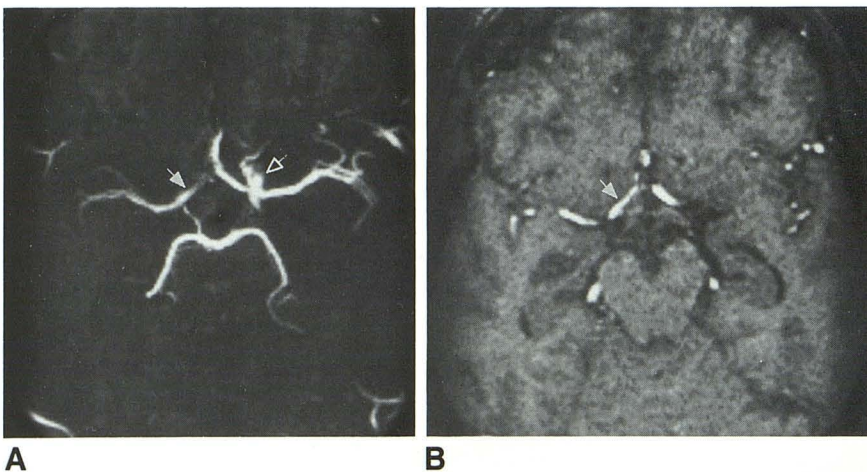
Second, the intensity of the background increases due to poor suppression of nonmoving protons. Suboptimal background suppression can be associated with TOF MRA because it is difficult to suppress completely the background tissue and optimize flow-related enhancement at the same time. For example, if one attempts to optimize background suppression by selecting a very short TR and a large flip angle, flow-related enhancement will diminish due to saturation effects and vessel contrast disappears. Therefore, compromises have to be made with all TOF protocols. In addition, if the background contains fat such as the skull base and carotid space, there may be poor suppression of fat signal due to the relative T1 weighting with some TOF sequences. This type of weighting arises from the use of spoiled gradient recalled sequences or the use of a very short TE (approximately 5 msec) which causes the fat signal to be in phase with respect to water protons at 1.5 T (16).

Third, if the amount of background within the projected volume is large, there will be a greater statistical chance that enough variations of the background intensity will occur. Therefore, a background voxel may have signal intensity higher than a voxel representing a vessel. If the ray-tracing algorithm passes through both voxels, vessel contrast will be lost since it is hidden by surrounding stationary tissue (Fig. 3).

Fig. 2. Comparison between source image and collapsed view in a patient status postocclusion of the right internal carotid artery.

A, Collapsed view of the circle of Willis (equivalent to a submental-vertex view) demonstrates lack of flow-related enhancement of the right internal carotid artery as compared to the normal left side (*open arrow*). There appears to be narrowing of the A1 segment of the right anterior cerebral artery (*solid arrow*).

B, Source image through this anterior cerebral artery (*arrow*) demonstrates that the diameter of this vessel was underestimated on the collapsed view.



### Overestimation of Stenosis and Pseudostenosis

Regions of true vessel narrowing will also be overestimated on the MIP reconstructions in a similar fashion to the loss of small vessel detail. For example, carotid stenosis will appear greater on the MIP reprojection when compared to the source image (Fig. 3). In addition, because of the sensitivity of MRA to regions of disturbed flow such as turbulence at a site of stenosis, additional signal loss will occur, resulting in overestimation of stenosis and false positives. This loss will be seen on the source images (Fig. 3D) as well and is accentuated on the resulting MIP reprojection (Fig. 3B). Turbulence results in overestimation of stenosis and leads to false positives on both source and MIP images.

Perhaps even more problematic are the regions of disturbed flow seen in normal vessels that can be mistaken for stenosis or vasospasm. Typical locations of pseudostenosis include the common carotid bifurcation, carotid siphon (Fig. 4), and terminal bifurcation of the internal carotid artery (Fig. 5). This narrowing will be accentuated on the MIP views when compared to the source images because of reduced vessel intensity.

### View-to-View Variations

Because MRA flow information is acquired from a volume of tissue, flow mapping from multiple view angles can be generated by rotating the direction of the ray-tracing algorithm, thus yielding a series of MIP reprojections. Since the quantity and intensity of background signal may be unevenly distributed around the vessel of interest, the MIP reprojection will have variable success in adequately depicting vascular anatomy. In some instances, different reprojections of



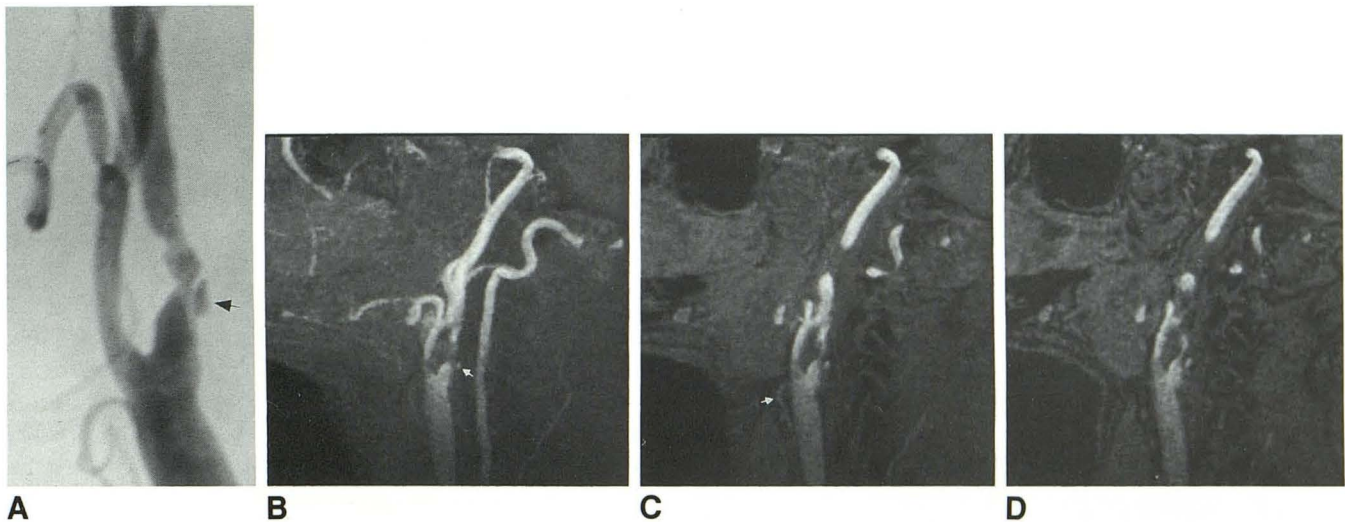


Fig. 3. Overestimation of stenosis when comparing between entire and limited volume MIP reprojections and source image in a patient with carotid bifurcation stenosis (3-D TOF MRA with sagittal-oriented source images).

A, Lateral x-ray angiogram depicts moderate to severe stenosis of the proximal internal carotid artery with ulceration (*arrow*).

B, Lateral MIP reconstruction of the entire sagittal 3-D volume through the lateral neck demonstrates underestimation of ulcer size (*arrow*). There is near complete loss of the vessel lumen distal to the ulcer leading to overestimation of the degree of stenosis.

C, Lateral MIP reconstruction edited to include only the sagittal source images through the carotid bifurcation. Note that improved morphologic detail is present because of the reduction of background material included in the reprojected volume. The superior thyroid artery (*arrow*) can now be visualized.

D, This unprocessed single-source image through the region of interest has the best vessel contrast and detail.

the same vessel(s) may appear quite different. An extreme case is depicted in Fig. 6.

### False Positives

The mechanisms involved in the generation of false positives are numerous. In some cases, a mismatch of intrinsic flow rates and the selected acquisition parameters is the primary culprit. For example, normal flowing blood will receive an excessive number of RF excitation pulses if the selected slab thickness for a 3-D TOF MRA is too large. As a result, saturation occurs with diminished flow-related enhancement of the vessels in the distal portion of the imaging volume (Fig. 7). Although less sensitive to saturation effects, 2-D TOF MRA may also show this artifact if the vessel is parallel to the plane of section. An example of this type of saturation occurs when performing multiple axial 2-D TOF sections through horizontal portions of the vertebral artery (Fig. 8).

Image processing and display can produce false positives. A common example is high signal from extravascular subacute thrombus, which appears hyperintense on the source images from a TOF acquisition. With MIP processing, these high signal regions are detected and incorporated into the reprojection making it difficult to distinguish between the clot and flowing blood (Fig. 9). In-

correct editing of the volume before applying the reprojection algorithm may also lead to erroneous results (Fig. 10).

### False Negatives

Although less common than false positives, a false negative collapsed or reprojected view may occur despite the fact that the finding is detected on the source image(s). This problem is most commonly encountered when the MIP emphasizes hyperintense signal from vessels at the expense of lower intensity structures, which may be of critical importance. For example, intraluminal thrombus or intimal flap may be obscured if surrounded by hyperintense flowing blood. Therefore, a perfectly normal vessel may be reconstructed; small defects are easily overlooked (Fig. 11).

### Vessel Overlap

The data obtained from an MRA may be thought of conceptually as being similar to an intravenous digital subtracted angiogram. That is, any flowing vessel within the region of interest may be opacified, or in the case of MRA, may register flow-related enhancement or phase shift. Vessel overlap may result. By editing the volume



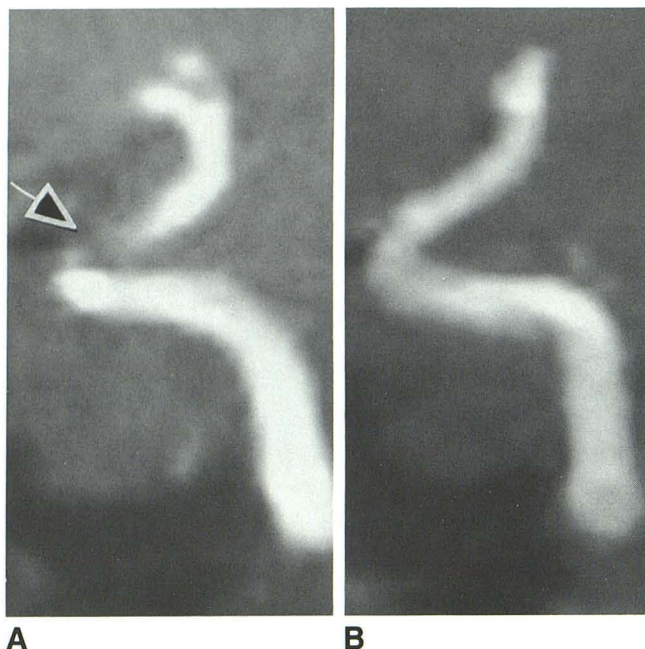


Fig. 4. Pseudostenosis of the carotid siphon in an 30-year-old healthy volunteer (3-D TOF MRA).

A, This lateral view of the siphon obtained using a TE of 7 msec demonstrates a region of possible narrowing (*arrow*). This degree of narrowing is overestimated on this MIP reprojection when compared to the source image (not shown). This signal loss within the carotid siphon on MRA is commonly seen at regions of disturbed flow associated with curved vascular structures and can be accentuated by longer TEs.

B, Same vessel and projection obtained with a shorter TE of 5 msec shows marked reduction of this artifact.

to isolate specific vessels, obtaining multiple re-projections, and inspecting the source images, vessel overlap will be less apparent.

## Solutions

A number of solutions are available to compensate for artifacts that can be grouped into four general categories: 1) optimize parameters, 2) edit volume size before performing MIP reconstructions, 3) refer to the individual source images, and 4) use alternative image processing.

### *Optimize Parameters*

There are several goals in protocol optimization including: 1) maximizing contrast differences between moving and stationary spins, 2) resolution, and 3) adequate coverage. Of these three, improving contrast is the most critical. Since signal loss in regions of disturbed flow is universal to all MRA techniques, the manufactures have gone to great lengths to reduce this artifact. For example,

all commercially available TOF and PC MRA software incorporate the shortest TE technically possible to reduce the effects of signal loss due to spin dephasing, field inhomogeneities, and/or susceptibility differences. In practical terms, the user may have either limited or no control of the selection of TE. Figure 4 is an example of the effect of adjusting the TE using experimental software.

In the case of TOF MRA, saturation is a major limiting factor resulting in vascular signal loss especially where slow flow is of interest (31). Therefore, if slow-flow states (such as dolichoectasia, presence of proximal arterial occlusion, slowly flowing giant aneurysms, arteriovenous malformations, or diminished cardiac output) are present, selecting a 2DFT instead of a 3DFT TOF MRA protocol is recommended. A 2DFT sequence will improve flow-related enhancement and reduce the potential of saturation by virtue of reducing the size of the area receiving RF pulses. Alternatively, if higher spatial resolution 3DFT TOF MRA is required, tailoring the parameters with concerns toward the anticipated reduced flow rates is necessary. For example, increasing the TR or reducing the flip angle up to a certain point can be incorporated into the protocol. The complex mechanisms involved with TR and flip angle on saturation and vessel visualization are beyond the scope of this paper but have been described in more detail elsewhere (26, 32, 33). An example of their influence is graphically shown on Figure 7.

Saturation effects due to slow flow are less problematic with PC MRA (Fig. 8). With PC MRA, poor image contrast due to slowly flowing vessels is related to the fact that the amount of detectable phase shift is proportional to velocity and vessel size in relation to the voxel volume. In slow-flow states, the degree of phase shift is reduced and may be difficult to resolve with the applied flow-encoding gradients. Some of these problems can be overcome by altering gradient waveforms or velocity encoding (34) which affects the range of velocity sensitivity. Specifying the exact velocity encoding, in cm/sec, requires some a priori knowledge of in vivo velocities. For example, a velocity encoding of 60 to 80 cm/sec might be appropriate for the intracranial segments of the internal carotid arteries but may be too high for the posterior circulation. If analysis of slowly flowing structures such as a giant aneurysm or dural sinus is required, a velocity encoding of 20 cm/sec would be more appropriate to have



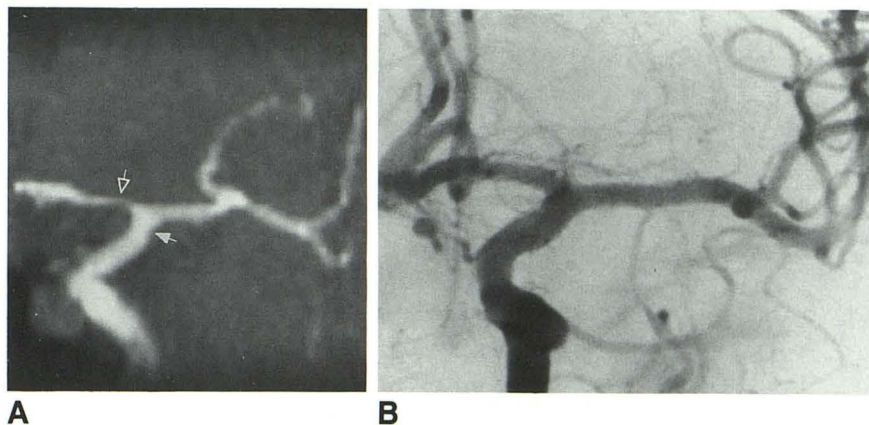


Fig. 5. Pseudostenosis in the region of distal internal carotid artery bifurcation (3-D TOF MRA).

A, The anterior-posterior MIP reconstruction of this region demonstrates apparent narrowing of the supraclinoid internal carotid artery (*solid arrow*) and proximal segment of the anterior cerebral artery (*open arrow*). These findings were less apparent on the source images (not shown).

B, Correlative x-ray angiography demonstrates no evidence of stenosis. The MRA findings were interpreted as signal loss due to disturbed flow.

enough phase shift sensitivity in the slow velocity range. To confirm arterial occlusion, an additional PC MRA may be performed at an even lower level of velocity encoding (5 cm/sec).

One drawback in using small velocity encoding values is the presence of aliasing artifact (34) which will occur if the actual velocities within the patient are greater than the user-defined velocity encoding. As a result, these higher velocities are greater than the prescribed phase shift range and can be misinterpreted as having a different velocity value or direction of flow. The resulting phase image will have regions of discontinuous signal drop out in normal vessels. If direction-sensitive reconstructions are produced, the expected direction of flow may be reversed (13). This type of aliasing artifact is somewhat analogous to what can be encountered with color flow Doppler imaging when high-velocity components may be incorrectly assigned a color-indicating flow in the opposite direction (35). There are additional problems encountered with PC MRA, including longer TE times, increased acquisition times when 3-D data sets are obtained, and increased reconstruction times.

Other factors in parameter optimization need to be mentioned. The addition of intravenous Gd-DTPA may be helpful in identifying small venous structures with TOF MRA. Unfortunately, greater vessel overlap and difficulties in trying to distinguish between small enhancing arteries and veins may be encountered. The cavernous segment of the internal carotid artery may be obscured because of enhancement of the surrounding cavernous sinus. There is also a potential for improving signal to noise with PC MRA following intravenous contrast administration.

Resolution, as expressed by voxel volume, may vary depending on the vessel of interest and the clinical question that needs to be addressed.

Voxel volumes about 1 cubic mm or greater may be sufficient for resolving carotid bifurcation disease, whereas sub cubic mm voxel is required for imaging the circle of Willis. Sub cubic mm voxel size will require the use of 3-D TOF or PC acquisitions with a resulting compromise in prolonged acquisition and reconstruction times, and reduced coverage per unit time when compared to a lower resolution 2-D acquisition.

Commercially available software packages allow some degree of freedom in user selection of TR, flip angle, and velocity encoding. Since these settings are independent variables and can be combined with other different options such as section or slab thickness and 2-D versus 3-D acquisition, all users will encounter difficulties in interpreting results in that either vessel morphology or visualization is different from anticipated. This problem arises from two sources. First, one is trying to obtain a functional flow map that may vary considerably with technique. Second, it is difficult to either quantitatively or qualitatively predict how each of these variables, when combined into a final protocol, can influence the study's final appearance (Fig. 7). Historically, MRA protocols were devised on an iterative trial-by-error basis in an attempt to minimize ambiguities and maximize vessel visualization. The beginning user can gain much by adopting these suggested protocols to serve as a starting point for clinical studies at his or her own site.

#### *Edit Volume Boundaries*

By limiting or editing the size of the volume before performing a MIP reconstruction, small vessel visualization can be improved and overestimation of stenosis can be reduced. Limiting the size of the volume minimizes the effect of background signal intensity fluctuation on the ray-



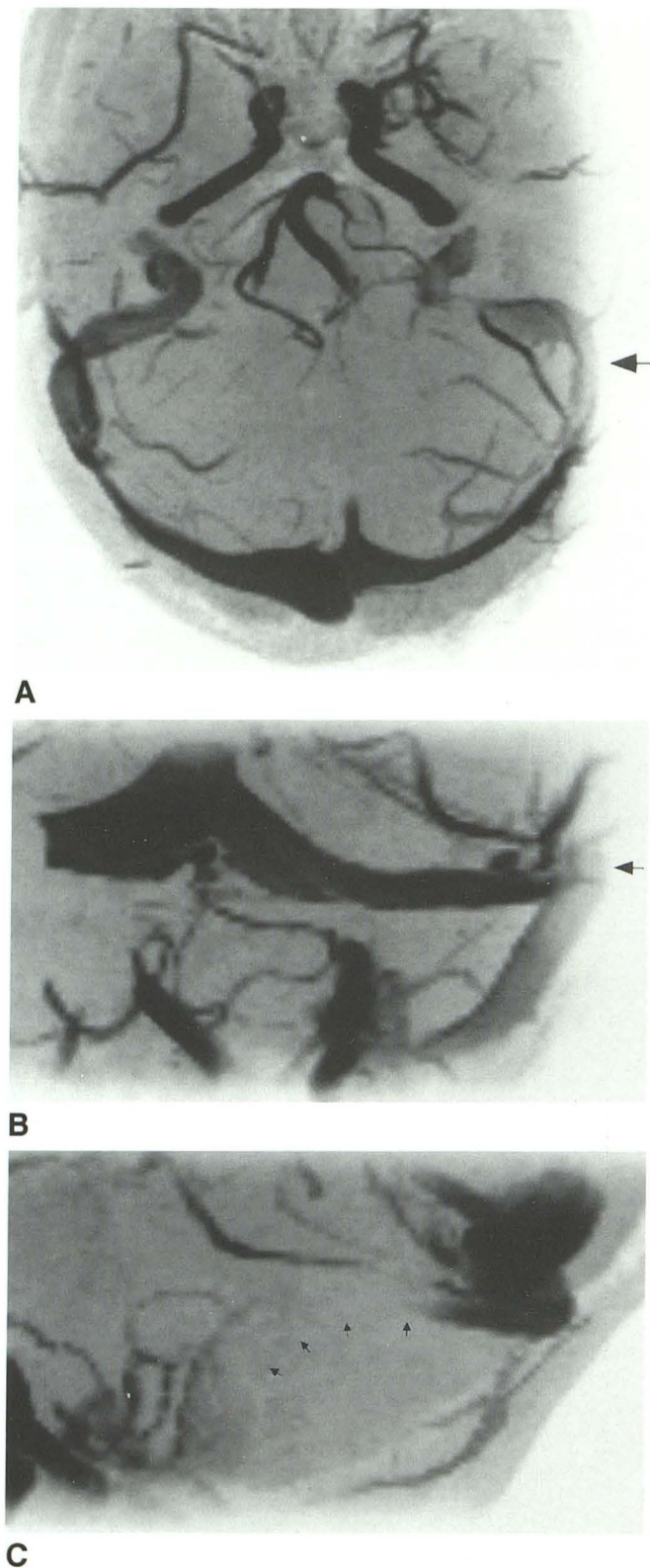


Fig. 6. View-to-view variations in vessel visibility due to the MIP reconstruction technique.

A, Collapsed 3-D TOF MRA of the posterior fossa in a normal patient. Because of the use of a rectangular field of view, that is narrower in the transverse axis, there is signal drop off along the

tracing procedure. Volume editing is more useful with TOF studies when compared to PC studies, since stationary tissue may have lower signal on PC MRA.

There are two methods for limiting the volume size. The first is to include only the source images that represent the region of interest. For example, if the carotid bifurcation is imaged using a 30-mm slab 3-D TOF MRA with 30, 1-mm thick sagittal sections, only a few critical sections actually encompass the lesion. The final MIP reconstruction can be markedly improved by using the minimum number of source images required when generating a sagittal collapsed view (Fig. 3C). This simple step can be easily performed on commercially available software.

A second editing method would be to reduce the area within each source image included in the final volume. For example, from the initial collapsed view, a region of interest can be drawn such that only the contents of that region are included. This type of editing is helpful when producing localized reprojections (Fig. 10). Care must be taken to ensure that the editing is performed properly to avoid unwanted vessel cutoff.

#### *Refer to the Individual Source Images*

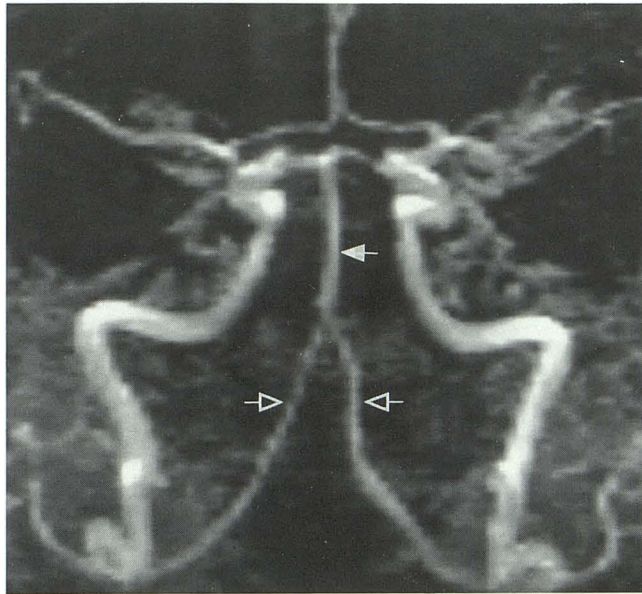
From the discussion above, it becomes evident that MIP reconstructions are inherently flawed. It makes sense, therefore, to review the "raw" unprocessed data or source images. At our institution, we place equal emphasis on viewing the source data and viewing the MIP reconstructions. The important information that can be gained is evident on Figures 2B, 3D, and 11A. Source images may be viewed on hard copy or on a work station. The source data also contains both

left lateral aspect of the brain including the left lateral transverse sinus (*arrow*).

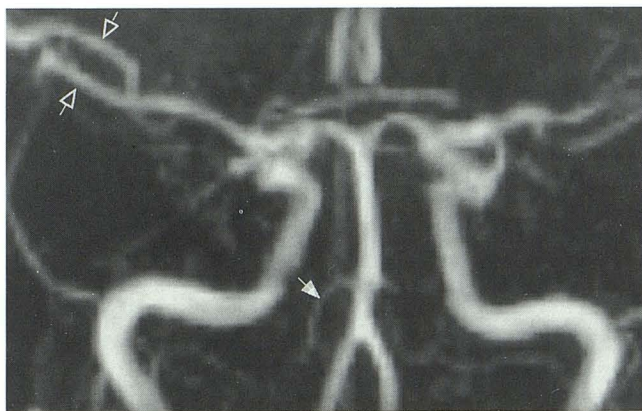
B, Anterior-posterior MIP reprojection of the left posterior fossa demonstrates an intact left transverse sinus. Note that the most lateral aspect of this sinus (*arrow*) is well seen since the background intensity anterior and posterior to this segment of the sinus is much more hypointense compared to the sinus.

C, Lateral reprojection of the left transverse sinus from the same region of interest as in B. In this reprojection, a major portion of the left transverse sinus is either absent or faintly seen (*arrows*). The reason for this "disappearing" sinus is due to the direction of the ray-tracing algorithm that is now oriented transversely to achieve a lateral view. Since the ray is required to pass through more hyperintense background including the center of the posterior fossa, there is a greater statistical chance that this background would be equal to the intensity of the lateral aspect of the transverse sinus. If the intensity of the background and vessel equalize, loss of this vascular segment will occur.





A



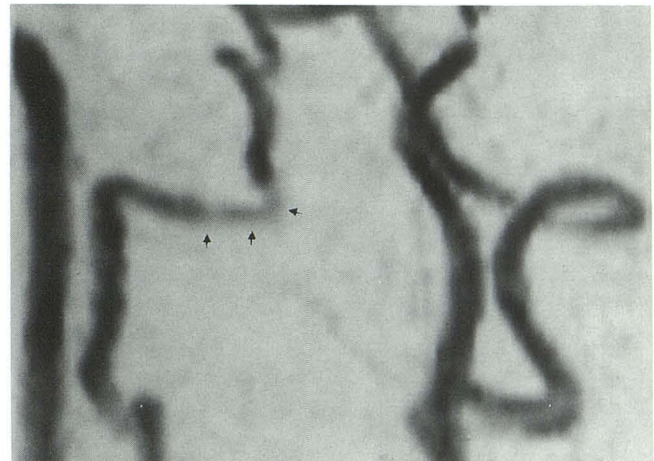
B

Fig. 7. Saturation as a function of acquisition parameters on a 3-D TOF MRA.

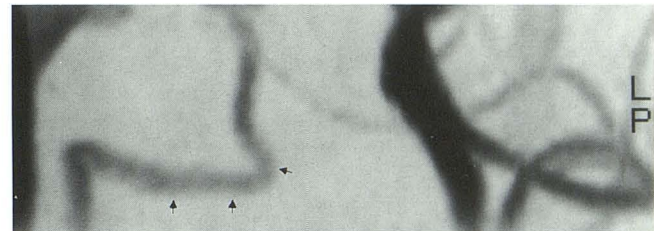
A, Anterior-posterior MIP reconstruction of the posterior circulation (TR 25 msec). Note the loss of vessel detail of the distal vertebral (*open arrows*) and basilar (*solid arrow*) arteries.

B, In the same patient, a repeat 3-D TOF MRA was performed (TR 50 msec) with the slab selection centered higher such that the distal vertebral arteries no longer receive RF pulses. Because all of these changes were made to reduce saturation, there is improved delineation of the posterior circulation. The right anterior inferior cerebellar artery is now visualized (*solid arrow*) and improved flow-related enhancement is also noted in the middle cerebral arteries (*open arrows*).

flow and anatomic information. Small structures, such as cranial nerves, can be visualized due to the inherent high resolution that is associated with MRA. In addition, the source images provide cross-sectional information, such as an aneurysm neck, that would be otherwise difficult to obtain on a catheter angiogram.



A



B

Fig. 8. Saturation effects due to in-plane flow simulating luminal narrowing.

A, Right anterior oblique MIP reconstruction from a multiaxial 2-D TOF MRA of the horizontal segment of the right cervical vertebral artery. There is subtle loss of signal and vessel caliber in this region (*arrows*) since this vessel segment is running within the axial plane of the source images resulting in partial saturation.

B, 3-D PC MRA (velocity encoding 40 cm/sec) of this same arterial segment shows normal vascular caliber (*arrows*). Since PC MRA is less sensitive to signal loss due to saturation, less reduction in vessel diameter is noted. Similar results might be expected from a 3-D TOF MRA since the degree of vessel saturation is relatively independent of vessel orientation within the imaging volume.

Signal loss due to metallic foreign bodies, such as from vascular clips following carotid endarterectomy, can also be easily detected on the source images. The origins of this type of signal loss will be less obvious on the MIP reconstructions since regions of pronounced signal loss will be masked by signal fluctuations in the surrounding tissue.

Reviewing the source information will not solve all problems. Both source data and MIP reconstructions may not be able to distinguish a lesion with T1 shortening such as subacute hemorrhage from flow-related enhancement (36, 37). Both may exhibit equal hyperintensity on TOF MRA exams and may lead to erroneous conclusions (Fig. 9). Correlation with a T1-weighted spin-echo study is helpful. PC MRA eliminates this source of confusion since flowing blood can be distin-



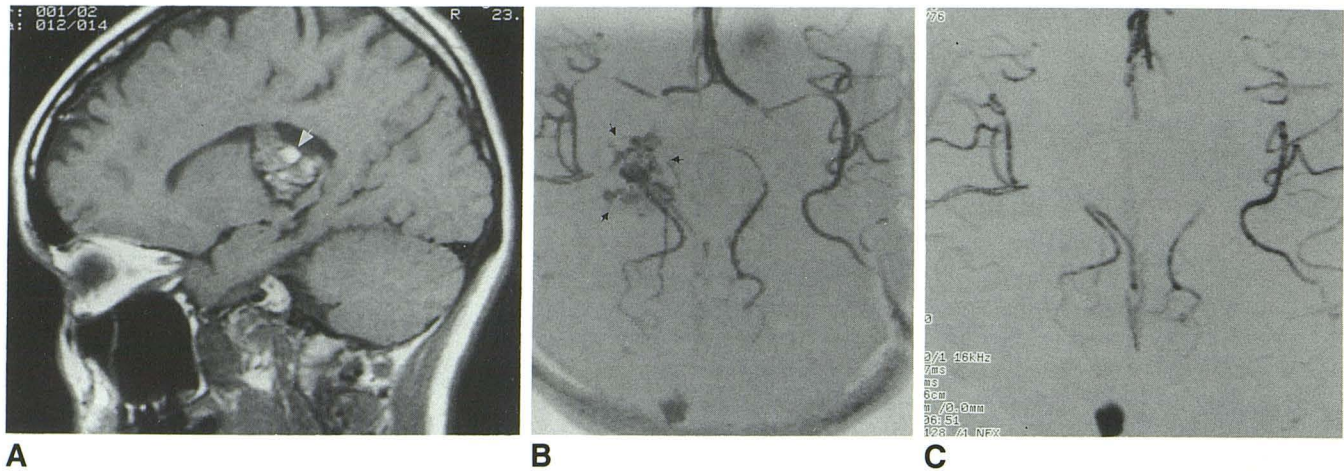


Fig. 9. False positive MIP reconstruction due to the presence of methemoglobin simulating flowing blood.  
 A, Parasagittal T1 spin-echo image demonstrates a cryptic malformation with evidence of multiple foci of subacute hemorrhage (arrow).  
 B, 3-D TOF MRA collapsed MIP view shows an irregular region of signal (arrows) generated by this hemorrhage that can be misinterpreted as a flowing vascular structure. The curvilinear artifact noted along the left side of the brain is due to aliasing.  
 C, 3-D PC MRA collapsed MIP view in the same region shows that the region of hemorrhage is no longer seen because of the lack of phase shift within the lesion. Note the improved background suppression with PC MRA which reflects the lack of phase shift of the stationary background material.

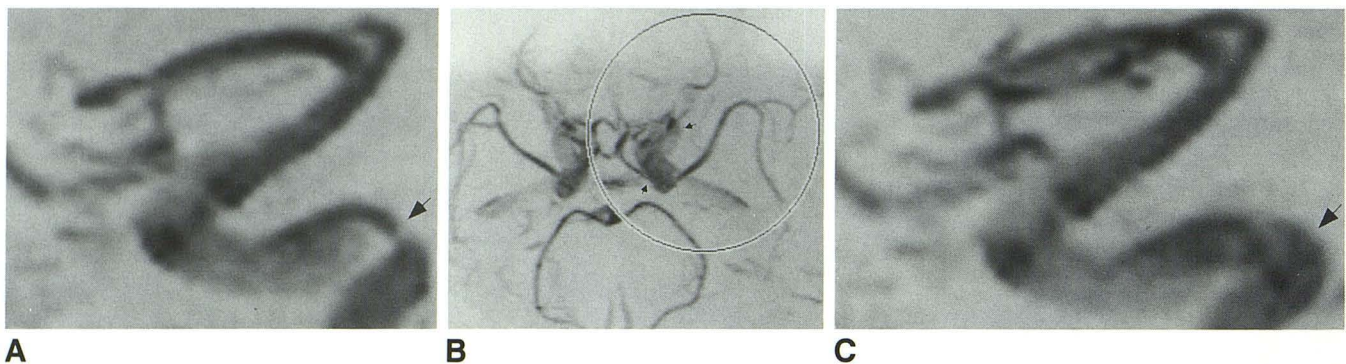


Fig. 10. Stenosis of the carotid siphon due to improper editing of the volume prior to MIP processing.  
 A, Lateral view of the carotid siphon from a 3-D TOF MRA demonstrates marked narrowing of the posterior cavernous segment of the internal carotid artery (arrow).  
 B, Because it was thought that the findings in A were due to a reconstruction artifact by not including the entire siphon within the volume that was reprojected, a new region of interest was drawn on the collapsed view. As shown by the circle, the entire siphon (arrows) is now included.  
 C, The new lateral reprojection now shows a normal appearing siphon.

guished from nonmoving thrombus because of the lack of associated phase shift.

#### *Use Alternative Image Processing*

Occasionally, neither source nor MIP images permit adequate vessel analysis. Difficulty in sorting out vascular anatomy due to inherent flaws in the MIP reconstruction may not be resolved on the source images if, for example, the vessel in question is sectioned at an oblique angle or if the disease process extends over several source images. An alternative approach is to view flow

information using multiplanar reconstruction (MPR) (16). MPR is essentially reconstruction of a single section taken from the imaging volume and oriented at an arbitrary angle such that it is different from the original plane of section of the source images. MPR reconstructions require interactive software for the operator to place graphically a plane of reconstruction through the vessel of interest. Commonly, an oblique orientation is selected and the new image is reconstructed with contrast and anatomic information that is similar to a source image. MPRs are occasionally per-



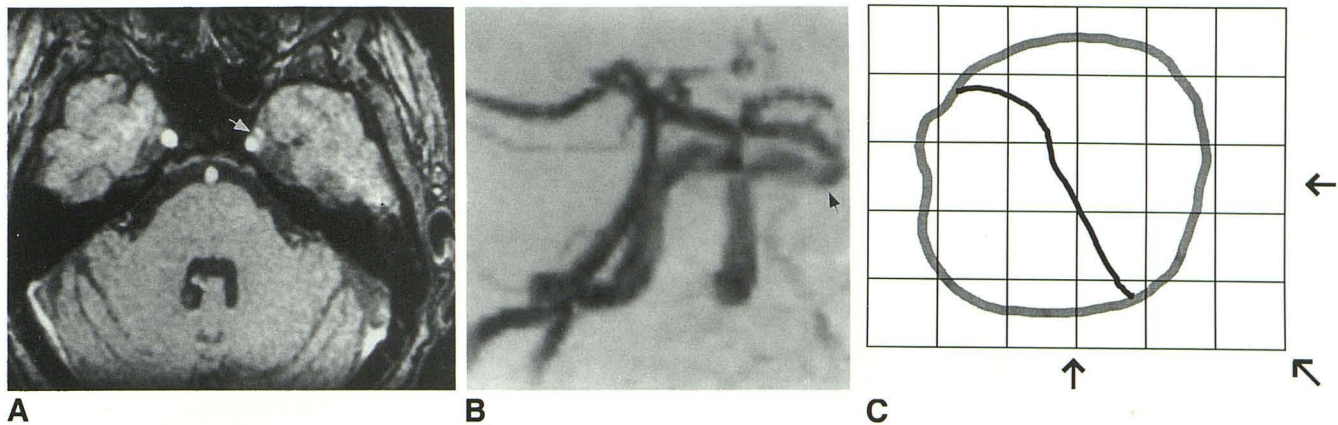


Fig. 11. A false negative MIP reprojection.

A, Source image through the skull base in a patient with a left hemisphere infarct depicts a carotid dissection with a relative hypointense intimal flap (*arrow*) extending between the regions of flow related enhancement in both the true and false lumens.

B, Oblique MIP reprojection of this carotid artery (*arrow*) shows no definite abnormality.

C, The reason for this false negative can be schematically shown on C. Both the true and false lumen correspond to voxels of marked hyperintensity. No matter what direction the ray-tracing algorithm is oriented (as indicated by the *arrows*) hyperintensity is encountered. Therefore, the hypointense intimal flap cannot be detected as a discrete structure on the final reprojection since only the maximum intensity voxel is displayed.

formed at our institution in regions where oblique single-section reconstructions are useful in depicting vascular and soft-tissue anatomy such as the aortic arch. Additional work comparing the utility of MPR as opposed to source images needs to be performed.

Proposals have been made to perform additional image manipulation on the source data that may reduce the need for the MIP algorithm. Connected component analysis is an example (30, 38). Since this type of reconstruction software is still regarded as a research tool and is not available for the majority of users, it will not be discussed any further.

## Summary

Neurovascular MRA will present new challenges because of its ability to gather functional information by the using novel techniques for acquisition, information processing, and display. By approaching artifact generation in the context of six major clinical problems, we have found that the underlying causes and solutions are easier to comprehend. Despite a more comprehensive understanding of the causes of artifact generation, and efforts by the manufacturers in providing timely software and hardware solutions, artifacts can be minimized, but not eliminated, in clinical studies. If equivocal findings are present, such as patient motion or flow saturation, definitive conclusions may not be possible. In these instances, other diagnostic tests are appropriate.

In addition, a negative MRA will not end the patient's diagnostic neurovascular work-up if there remains strong clinical evidence of neurovascular disease, since the overall reliability and accuracy of MRA has not been defined.

## Acknowledgment

We thank Charles Anderson for providing some of the figures.

## References

1. Laub GA, Kaiser WA. MR angiography with gradient motion refocusing. *J Comput Assist Tomogr* 1988;12:377-382
2. Dumoulin CL, Souza SP, Walker MF, Wagle W. Three-dimensional phase contrast angiography. *Magn Reson Med* 1989;9:139-149
3. Gullberg GT, Wehrli FW, Shimakawa A, Simons MA. MR vascular imaging with a fast gradient refocused pulse sequence and reformed images from transaxial sections. *Radiology* 1987;165:241-246
4. Keller PJ, Drayer BP, Fram EK, Williams KD, Dumoulin CL, Souza SP. MR angiography with two-dimensional acquisition and three-dimensional display: work in progress. *Radiology* 1989;173:527
5. Masaryk TJ, Modic MT, Ross JS, et al. Intracranial circulation: preliminary clinical results with three-dimensional (volume) MR angiography. *Radiology* 1989;171:793-799
6. Mattle HP, Wentz KU, Edelman RR, et al. Cerebral venography with MR. *Radiology* 1991;178:453-458
7. Litt AW, Eidelman EM, Pinto RS, et al. Diagnosis of carotid artery stenosis: comparison of 2DFT time-of-flight MR angiography with contrast angiography in 50 patients. *AJNR* 1991;12:149-154
8. Masaryk TJ, Modic MT, Ruggieri PM, et al. Three-dimensional (volume) gradient-echo imaging of the carotid bifurcation: preliminary clinical experience. *Radiology* 1989;171:801-806
9. Masaryk AM, Ross JS, DiCello MC, Modic MT, Paranandi L, Masaryk TJ. 3DFT MR angiography of the carotid bifurcation: potential and



- limitations as a screening examination. *Radiology* 1991;179:797-804
10. Ross JS, Masaryk TJ, Modic MT, Harik SI, Wiznitzer M, Selman WR. Magnetic resonance angiography of the extracranial carotid arteries and intracranial vessels: a review. *Neurology* 1989;39:1369-1376
  11. Ross JS, Masaryk TJ, Modic MT, Ruggieri PM, Haacke EM, Selman WR. Intracranial aneurysms: evaluation by MR angiography. *AJNR* 1990;11:449-456
  12. Sevick RJ, Tsuruda JS, Schmalbrock P. Use of 3D time of flight magnetic resonance angiography in the evaluation of intracranial aneurysms. *J Comput Assist Tomogr* 1990;14:874-881
  13. Tsuruda JS, Shimakawa A, Pelc NJ, Saloner D. Dural sinus occlusion: evaluation with phase-sensitive gradient-echo MR imaging. *AJNR* 1991;12:481-488
  14. Edelman RR, Wentz KU, Mattle HP, et al. Intracerebral arteriovenous malformations: evaluation with selective MR angiography and venography. *Radiology* 1989;173:831
  15. Anderson CM, Saloner D, Tsuruda JS, Shapeero LG, Lee RE. Artifacts in maximum-intensity-projection display of MR angiograms. *AJR* 1990;154:623-629
  16. Lin W, Haacke EM, Smith AS. Lumen definition in MR angiography. *J Magn Reson Imaging*. 1991;1:327-336
  17. Lenz GW, Haacke EM, Masaryk TJ, Laub GA. In-plane vascular imaging: pulse sequence design and strategy. *Radiology* 1988;166:875-882
  18. Dumoulin CL, Cline HE, Souza SP, Wagle W, Walker MF. Three-dimensional time-of-flight magnetic resonance angiography using spin saturation. *Magn Reson Med* 1989;11:35-46
  19. Nishimura DG. Time-of-flight angiography. *Magn Reson Med* 1990 14:194-202
  20. Axel L, Morton D. MR flow imaging by velocity-compensated/uncompensated difference images. *J Comput Assist Tomogr* 1987;11:31-34
  21. Pernicone JR, Siebert JE, Potchen EJ, Pera A, Dumoulin CL, Souza SP. Three-dimensional phase-contrast MR angiography of the head and neck: preliminary report. *AJNR* 1990;11:457-466
  22. Rosnick S, Laub G, Braekle R. *Three dimensional display of blood vessels in MRI*. Paper presented at Proceedings of the IEEE Computers in Cardiology, New York, 1986
  23. Laub G. Displays for MR angiography. *Magn Reson Med* 1990;14:222-229
  24. von Schulthess GK, Higgins CB. Blood flow imaging with MR: spin-phase phenomena. *Radiology* 1985;157:687-695
  25. Podolak MJ, Hedlund LW, Evans AJ, Herfkens RJ. Evaluation of flow through simulated vascular stenoses with gradient echo magnetic resonance imaging. *Invest Radiol* 1989;24:184-189
  26. Haacke EM, Masaryk TJ, Wielopolski PA, et al. Optimizing blood vessel contrast in fast three-dimensional MRI. *Magn Reson Med* 1990;14:202-221
  27. Motomiya M, Karino T. Flow patterns in human carotid artery bifurcation. *Stroke* 1984;15:50-56
  28. Caro CG, Parker KH. Mechanics and imaging of the macrocirculation. *Magn Reson Med* 1990;14:179-186
  29. Ehman RL, Felmlee JP. Flow artifact reduction in MRI: a review of the roles of gradient moment nulling and spatial presaturation. *Magn Reson Med* 1990;14:293-307
  30. Cline H, Dumoulin CL, Lorensen WE, Souza SP, Adams WJ. Volume rendering and connectivity algorithms for MR angiography. *Magn Reson Med* 1991;18:385-394
  31. Wehrli FW. Time-of-flight effects in MR imaging of flow. *Magn Reson Med* 1990;14:187-193
  32. Marchal G, Bosmans H, Van Fraeyenhoven L, et al. Intracranial vascular lesions: optimization and clinical evaluation of three-dimensional time-of-flight MR angiography. *Radiology* 1990;175:443-448
  33. Ruggieri P, Laub G, Masaryk T, Modic M. Intracranial circulation: pulse sequence considerations in three dimensional (volume) MR angiography. *Radiology* 1989;171:785-791
  34. Spritzer CE, Pelc NJ, Lee JN, Evans AJ, Sostman HD, Riederer SJ. Rapid MR imaging of blood flow with a phase-sensitive, limited-flip-angle, gradient recalled pulse sequence: preliminary experience. *Radiology* 1990;176:255-262
  35. Mitchell DG. Color Doppler imaging: Principles, limitations, and artifacts. *Radiology* 1990;177:1-10
  36. Yousem DM, Balakrishnan J, Debrun GM, Bryan RN. Hyperintense thrombus on GRASS MR images: potential pitfall in flow evaluation. *AJNR* 1990;11:51-58
  37. Tsuruda JS, Halbach VV, Higashida RT, Mark AS, Hieshima GB, Norman D. MR evaluation of large intracranial aneurysms using cine low flip angle gradient-refocused imaging. *AJNR* 1988;9:415-424
  38. Saloner D, Hanson WA, Tsuruda JS, van Tyen R, Anderson CM, Lee RE. The application of a connected voxel algorithm to magnetic resonance angiographic data. *J Magn Reson Imaging* 1991;1:423-430